Neutron spectroscopy with the Spherical Proportional Counter

E. Bougamont[a], A. Dastgheibi[a], J. Derre[a], J. Galan[a], G. Gerbier[b], I. Giomataris[a], M. Gros[a], I. Katsioulas[c], D. Jourde[a], P. Magnier[a], X.F. Navick[a], T. Papaevangelou[a], I. Savvidis[c], G. Tsiledakis[a]

[a] *IRFU, Centre d'etudes de Saclay, Gif sur Yvette, France*
[b] *Queens University, Kingston, Canada*
[c] *Aristotle University of Thessaloniki, Thessaloniki, Greece*

arXiv:1512.04346v1 [physics.ins-det] 14 Dec 2015

Abstract

A novel large volume spherical proportional counter, recently developed, is used for neutron measurements. Gas mixtures of N_2 with C_2H_6 and pure N_2 are studied for thermal and fast neutron detection, providing a new way for the neutron spectroscopy. The neutrons are detected via the $^{14}N(n,p)C^{14}$ and $^{14}N(n,\alpha)B^{11}$ reactions. Here we provide studies of the optimum gas mixture, the gas pressure and the most appropriate high voltage supply on the sensor of the detector in order to achieve the maximum amplification and better resolution. The detector is tested for thermal and fast neutrons detection with a ^{252}Cf and a $^{241}Am-^{9}Be$ neutron source. The atmospheric neutrons are successfully measured from thermal up to several MeV, well separated from the cosmic ray background. A comparison of the spherical proportional counter with the current available neutron counters is also given.

1. Introduction

The Spherical Proportional Counter is a novel concept with very promising features, among which is the possibility of easily instrumenting large target masses with good energy resolution and low energy threshold. The natural radial focusing of the spherical geometry allows collecting and amplifying the deposited charges by a simple and robust detector using a single electronic channel to read out a large gaseous [1, 2, 3]. The sensitivity of the detector is obtained by using the Rn daughters decay for alpha particles in the energy range of 5.3 - 7.7 MeV. The low energy calibration of the detector from 100 eV up to several tenths of keV is achieved by using X-rays and a UV lamp [4, 5]. The detector has been successfully used as a neutron detector based on the $^3He(n,p)H^3$ reaction. At the present work the spherical proportional counter has been optimized for operation in pure Nitrogen (N_2), which presents an interesting neutron converter, permitting neutron spectroscopy up to 20 MeV. The thermal and fast neutrons are detected via the $^{14}N(n,p)C^{14}$ reaction and the fast neutrons with energy greater than 1.7 MeV via the$^{14}N(n,\alpha)B^{11}$ reaction. The low background of the detector and the possibility to separate the γ ray pulses from the proton and alpha particle pulses (through pulse shape analysis) increase the sensitivity for the neutron detection. The detector can successfully measure very low thermal neutron fluxes, giving the possibility for neutron energy spectrum up to several MeV at ground and underground level [6].

2. The detector

The detector consists of a large spherical copper vessel, 1.3 m in diameter and 6 mm thick. The spherical vessel is well pumped (up to 10^{-8} $mbar$) and then filled with a gas mixture at a pressure from several hundreds of mbar up to 5 bar. An outgassing in the order of 10^{-9} $mbar/s$ is necessary for the amplification stability, because the presence of the O_2 in the drift volume induces electron attachment. A small stainless ball, usually of 14 mm in diameter, is fixed in the center of the spherical vessel by a stainless steel rod, acts as an electrode with positive high voltage and as a proportional amplification counter. In order to fulfill the requirements for operation with pure N_2 the 14 mm ball has been replaced by a smaller 8 mm and 3 mm ball. In addition, to reduce negative effects of occasional sparks the metallic ball has been successfully

replaced by a silicon ball. These improvements were necessary to achieve proportional amplification in pure N_2, a process occurring at extremely high electric fields. Figure 1 shows a typical spectrum produced by a ^{55}Fe source at 500 mbar N_2 pressure, the obtained resolution (σ) is reasonably good at about 10%.

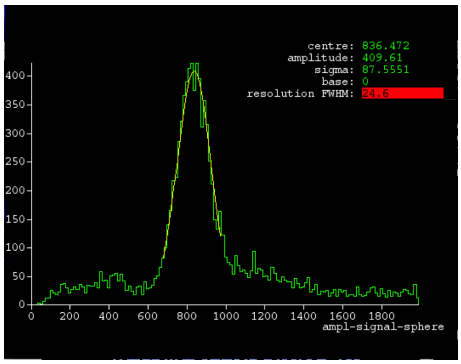

Figure 1: Spectrum of the ^{55}Fe source obtained with the spherical detector filled with Nitrogen (N_2) gas at 500 mbar.

3. The neutron detection

The detector is filled with gas mixtures of $N_2 + C_2H_6$ or with pure N_2 at pressure up to 500 mbar were the neutrons interact with the ^{14}N nucleus via the

$$^{14}N + n \rightarrow {}^{14}C + p + 625.87keV$$

reaction.

The energy of the exothermic reaction is shared between the ^{14}C and the proton with $E_C = 41.72$ keV and $E_p = 584.15$ keV in the case of thermal neutrons. The cross section for thermal neutrons is 1.83 barn and for fast neutrons is shown in figure 2. Because of their energy and their long range in the gas mixture, the protons play the main role for signal characteristics such as the risetime and the width. A ^{252}Cf neutron source on the top of the sphere has been used for thermal and fast neutron detection. Fast neutrons can be well detected also via the

$$^{14}N + n \rightarrow {}^{11}B + \alpha - 158keV$$

reaction up to $E_n = 20$ MeV.

This endothermic reaction plays a dominant role in the fast neutron detection for an incident neutron energy greater than 1.7 MeV, since the cross section of the $^{14}N(n,\alpha)B^{11}$ reaction is higher than that of the $^{14}N(n,p)C^{14}$ reaction.

Figure 3 shows the neutron data from the detector, with gas mixture N_2 (200 mbar) and C_2H_6 (10 mbar), irradiated with ^{252}Cf source. The thermal neutron signals are given in the peak of 625.87 keV and come only from the $^{14}N(n,p)C^{14}$ reactions, well separated from the cosmic rays and the recoils. Thus, the calculation of the thermal neutron flux becomes an easy task. The fast neutron signals are at the right of the thermal neutron peak, produced from both the (n,p) and the (n,a) reactions. In the left picture of the figure 3 the scatter plot of the risetime of the signal (which actually provides the depth of the ionization electrons produced in the gas) is presented as a function of the amplitude and in the right picture is the amplitude spectrum in ADC units. The recoil nuclei, which are produced from the fast neutron scattering, produce the low energy signals.

The atmospheric neutrons have been also successfully measured with pure N_2 at 500 mbar. The thermal neutron peak and the fast neutrons are presented in figure 4 after 15 hours of acquisition.

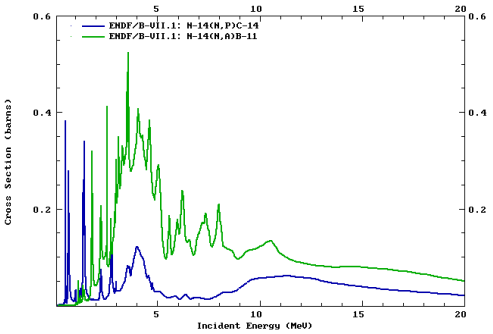

Figure 2: The cross sections of the reactions $^{14}N(n,\alpha)B^{11}$ and $^{14}N(n,p)C^{14}$ for neutrons of energy up to 20 MeV.

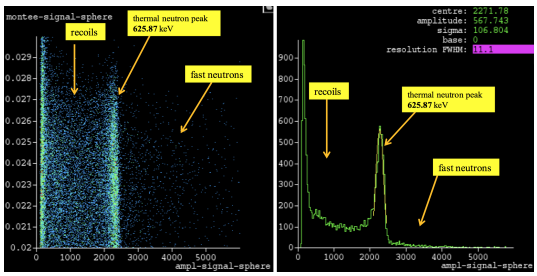

Figure 3: Neutrons from a ^{252}Cf source. In the left picture is the rise time as a function of the amplitude and in the right picture is the amplitude spectrum in ADC units.

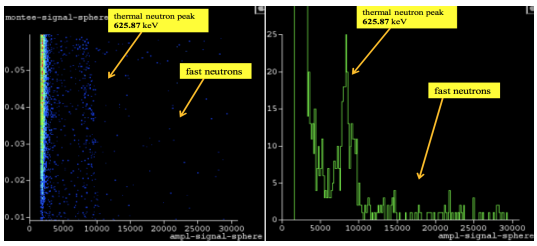

Figure 4: Atmospheric neutron detection with 500 mbar pure N_2 gas. In the left picture is the risetime as a function of the amplitude and in the right picture is the amplitude spectrum in ADC units.

4. Fast neutrons from ^{252}Cf and $^{241}Am-^{9}Be$ neutron sources and the limitation of the wall effect

Long irradiation time measurements with ^{252}Cf $(6.4 \cdot 10^4\ Bq)$ and $^{241}Am-^{9}Be$ $(6.0 \cdot 10^4\ Bq)$ neutron sources have been done, to study fast neutron detection and the limitation due to wall effect. In figure 5 we present the experimental energy distribution of the signals (left picture), produced by the fast neutrons of the ^{252}Cf (right picture). A sensor with silicon, ball 3 mm in diameter, had been used in 400 mbars pure N_2. The ^{252}Cf neutrons have a distribution with a maximum close to 1.4 MeV. The experimental distribution of the events depends mainly on the neutron cross sections and on the wall effect. In the energy range of the ^{252}Cf neutrons, the (n,p) reactions play a dominating role (figure 2). In the spectrum we see the characteristic (n,p) cross section peaks and the accumulation of the signals at lower energies because of the wall effect.

In the figure 6 (left picture) we present the experimental data after irradiation with $^{241}Am-^{9}Be$ neutron source using a sensor of 8 mm metallic ball and N_2 gas filling at 200 mbar. Since the neutrons of a $^{241}Am-^{9}Be$ source (figure 6, (right picture) have higher energy compared to the neutrons of a ^{252}Cf source, most events are coming from the (n,a) reaction. As in the previous figure, we can see the accumulation

Experimental data from ^{252}Cf neutron source irradiation, 3 mm sensor, N_2 gas filling at 400 mbar.

^{252}Cf source neutron energy spectrum .

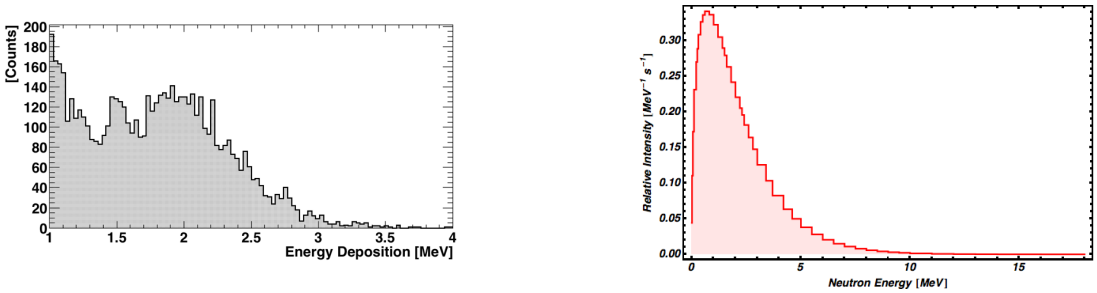

Figure 5: Experimental data after irradiation with ^{252}Cf neutron source. The (n,p) cross sections coincidence peaks appear at the left picture.

of the signals at lower energy because of the wall effect and the neutron moderation by the surrounding materials.

Experimental data from $^{241}Am-^{9}Be$ neutron source irradiation, 8 mm sensor, Nitrogen (N_2) gas filling at 200 mbar.

$^{241}Am-^{9}Be$ source neutron energy spectrum.

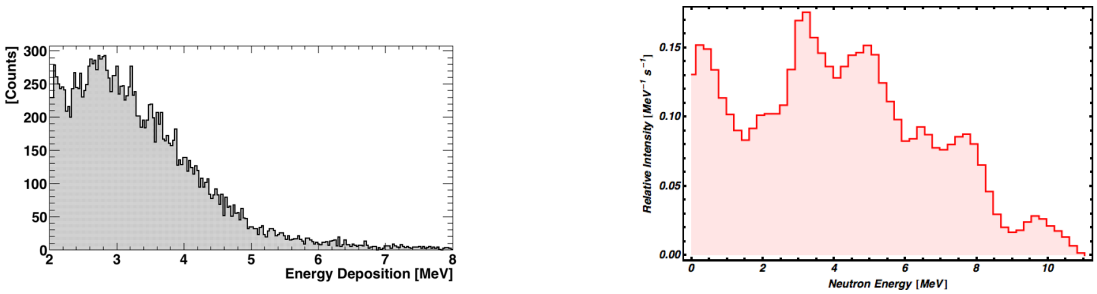

Figure 6: Experimental data after irradiation with $^{241}Am-^{9}Be$ neutron source. There is translation of the spectrum to the left because of the wall effect.

In order to measure the neutron energy, the produced charged particles from both (n,p) and (n,a) reactions must deposit all their energy in the drift volume. If the reaction takes place close to the vessel wall, it is possible for one of the charged particles or both of them to hit the wall and to lose a part of their energy. This is known as the wall effect and leads to wrong estimation of the neutron energy. In the case of the detector being used as a neutron spectrometer and not as a simple neutron counter, the wall effect plays an important role. The wall effect depends on the ranges of the produced particles in the drift volume and on the size of the detector. In figure 7 we present the wall effect of the sphere as a function of the sum of the ranges of the produced charged particles. The range of $^{14}C^{+}$ and the range of protons in the case of the (n,p) reactions, the range of $^{11}B^{+}$ and the range of alphas for the (n,a) reactions. The ranges depend on the neutron energy and on the gas pressure. As an example for pure N_2 gas at 500 mbar pressure, the proton range for thermal neutrons is 2.2 cm and the wall effect 2%. The $^{14}C^{+}$ range is very low compared with that of the protons (250 μm for the thermal neutrons). The wall effect is more important for the fast neutrons since the range of 1.5 MeV protons is 8.7 cm in the same gas mixture at 500 mbar and the wall effect 10%. For neutron energies higher than 2 MeV the $^{14}N(n,a)B^{11}$ reaction is the dominant one for the fast neutron detection. As an example, the ranges of the ^{11}B and the a particles in 500 mbar N_2 for 4 MeV neutrons are approximately 0.7 cm and 3 cm respectively and the wall effect is 4%.

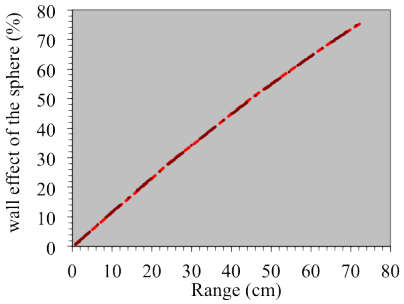

Figure 7: The wall effect of the SPC as a function of the sum of the ranges of the ^{14}C and the p.

5. Comparison with the commercial neutron counters.

There are many commercially available neutron counters mainly in cylindrical shape, with different diameters and lengths. The tubes are filled with ^3He gas or $^{10}BF_3$ gas and the neutrons are detected via the $^3He(n,p)H^3$ and $^{10}B(n,a)Li^7$ reactions. Both counter types, are very sensitive to thermal neutrons because of the positive Q-values and the high cross sections.

$$^3He(n,p)H^3\text{: } Q = 0.76\ MeV \text{ and } \sigma_{th} = 5330\ barn$$

$$^{10}B(n,a)Li^7\text{: } Q = 2.79\ MeV \text{ and } \sigma_{th} = 3837\ barn\ (6\%)$$

$$^{10}B(n,a)Li^{*7}\text{: } Q = 2.31\ MeV \text{ and } \sigma_{th} = 3837\ barn\ (94\%),\ ^7Li^* \rightarrow {}^7Li + 480\ keV$$

In comparison with the ^3He and $^{10}BF_3$, the N_2 has lower cross section for thermal neutrons ($\sigma = 1.83$ barn) but this disadvantage can be covered sufficiently by the large amount of nitrogen atoms in the sphere. Thanks to the large volume of the sphere the wall effect is very small compared with that of the cylindrical tubes. Additionally the cost of the ^3He gas is very high and the $^{10}BF_3$ is very toxic gas. For the fast neutrons up to 20 MeV the three isotopes, ^3He, $^{10}BF_3$ and ^{14}N, have comparable cross sections (figure 8), but the large volume of the spherical detector (1 m^3) with the large amount of N_2 gas (up to 500 mbar) inside, gives the possibility for direct fast neutron spectroscopy. The use of ^3He instead of N_2 in the spherical proportional counter is also suitable for fast neutron spectroscopy, but the high cost of the ^3He gas is a big disadvantage. In a polyenergetic neutron field (thermal and fast neutrons) the ^3He fast neutron recoils give similar signals with those of the 0.76 MeV thermal neutron peak, increasing the background. Both the ^3He and the$^{10}BF_3$ counters can be used for fast neutron detection but with the help of moderators.

6. Future developments

The first test measurements have shown the capabilities of the spherical detector as a neutron counter based on N_2 and have revealed its potential as a simple neutron spectrometer. The performance of the detector is expected to improve in the coming tests by applying the following changes:

- operation in higher gas pressure, thus increasing the detection efficiency and minimizing at the same time the wall effect
- reduce the diameter of the electrode ball
- use mixtures of N_2 with heavy gasses like Ar and Xe. The addition of those gasses will reduce the range of the reaction products, limiting the wall effect

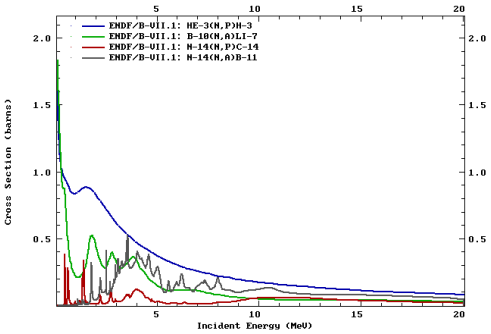

Figure 8: Comparison of the cross sections of the reactions $^3He(n,p)H^3$, $^{10}B(n,a)Li^7$, $^{14}N(n,p)C^{14}$ and $^{14}N(n,a)B^{11}$ for fast neutrons of energy up to 20 MeV.

On going simulations show that particle discrimination through pulse shape analysis technique is possible. The separation is based on the fact that the proton range in the gas is longer than the one of alpha particles of the same energy, which reflects to larger risetimes as it can be seen in figure 9. Identifying (n,p) from (n,a) reactions will simplify the neutron spectrum reconstruction. Furthermore, the wall effect is much less important for the (n,a) reactions, so it is expected to extend the range of the spectroscopy to higher neutron energies.

In order to exploit the spectroscopy capabilities of the spherical detector we are planning a series of measurements with monoenergetic neutron beams in facilities like CEA Cadarache or N.C.S.R. Athens.

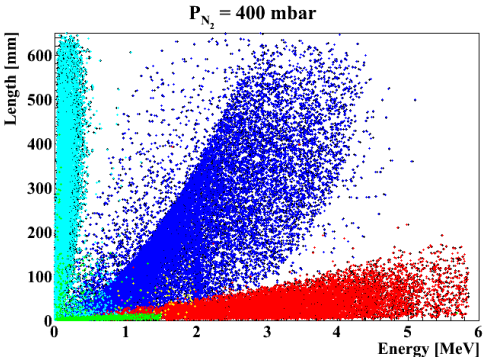

Figure 9: Particle range as a function of the deposited energy for 400 mbar N_2. Red corresponds to alphas and blue to protons. Other events are noted as green and light blue.

7. Conclusions

The spherical proportional counter can be used successfully as a neutron detector via the $^{14}N(n,p)C^{14}$ and $^{14}N(n,a)B^{11}$ reactions. Both gasses N_2 with C_2H_6 and the pure N_2 are performing well. The large volume with the possibility to operate at high gas pressure is an important advantage of our detector compared to the typical cylindrical proportional counters. This new concept has been proven to operate in a simple and robust way being efficient for neutron spectroscopy up to 20 MeV with minimized wall effect. The thermal neutron flux from the ^{252}Cf source (with moderator) and from the atmosphere have been precisely measured and the fast neutrons from the source and the atmosphere have been well detected.

References

[1] *I. Giomataris and J.D. Vergados*, Neutrino properties studied with a triton source and a large spherical TPC, Nuclear Instruments and Methods in Physics Research Section A: Accelerators, Spectrometers, Detectors and Associated Equipment, Volume 530, Issue 3, 11 September 2004, Pages 330-358, ISSN 0168-9002, http://dx.doi.org/10.1016/j.nima.2004.04.223. (http://www.sciencedirect.com/science/article/pii/S016890020401071X)

[2] *I. Giomataris et al*, NOSTOS experiment and new trends in rare event detection. Nuclear Physics B - Proceedings Supplements, 150:208 213, 2006. ISSN 0920-5632. doi: http://dx.doi.org/10.1016/j.nuclphysbps.2005.01.245. URL http://www.sciencedirect.com/science/article/pii/S0920563205008431.

[3] *S. Aune et al*, AIP Conf.Proc. 785 (2005) 1108.

[4] *I. Giomataris et al*, JINST 3 (2008) P09007. doi:10.1088/1748-0221/3/09/P09007. arXiv:0807.2802.

[5] *S. Andriamonje et al*, J. Phys. Conf. Ser. 179 (2009) 012003. doi:10.1088/1742-6596/179/1/012003.

[6] *I. Savvidis et al*, TAUP Conference 785 (2009) 1108.

European Union
European Social Fund

OPERATIONAL PROGRAMME
EDUCATION AND LIFELONG LEARNING
investing in knowledge society
MINISTRY OF EDUCATION & RELIGIOUS AFFAIRS
MANAGING AUTHORITY

NSRF 2007-2013
programme for development
EUROPEAN SOCIAL FUND

Co-financed by Greece and the European Union